ELSEVIER

Seminars in
NUCLEAR
MEDICINE

Optimized Scintigraphic Evaluation of Infection and Inflammation: Role of Single-Photon Emission Computed Tomography/Computed Tomography Fusion Imaging

Tira Bunyaviroch, MD, Atul Aggarwal, MD, and M. Elizabeth Oates, MD

Gallium-67 citrate and radiolabeled white blood cells have become standard inflammation/infection-seeking agents whereas other agents, such as ^{99m}Tc diphosphonates, commonly are used to infer an infectious process. These radiopharmaceuticals reflect physiologic and pathologic function rather than anatomical abnormality. In the clinical setting, it is often necessary to correlate these functional studies with anatomical imaging. The advent of single-photon emission computed tomography, as well as positron emission tomography, provides tomographic images for direct correlation to anatomic modalities such as computed tomography and magnetic resonance imaging. The methods by which these functional and anatomic imaging modalities are correlated include side-by-side, software, and hardware fusion. Clinically, fusion imaging has been applied primarily to oncologic and neurologic applications. The literature supports the premise that multimodality fusion would increase the specificity of the physiologic modality and increase the sensitivity of the anatomic modality. Our institution uses software fusion to aid in the diagnosis of infection and inflammation. Through case vignettes, we illustrate applications for single-photon emission computed tomography/computed tomography fusion for the diagnosis of infection and inflammation in multiple organ systems.
Semin Nucl Med 36:295-311

Radiopharmaceuticals for the detection and localization of infectious and inflammatory processes have been investigated since the 1950s.[1,2] Two of the well-known infection/inflammation-seeking agents are gallium-67 (^{67}Ga) and radiolabeled white blood cells (WBCs). Other agents such as technetium-99m (^{99m}Tc) diphosphonates have been used to infer inflammatory processes. Newer agents such as radiolabeled monoclonal antibodies, radiolabeled ciprofloxacin, and ^{18}F-fluorodeoxyglucose (FDG) have the potential for faster and more specific diagnosis.

It is well known that these radiotracers reflect function rather than anatomy. Although gross anatomic detail can be inferred from nuclear images, fine anatomic detail can make critical differences in diagnostic accuracy by facilitating the discrimination of physiologic from pathologic radiotracer localization. As will be discussed further, techniques for integrating functional and anatomic information, notably single-photon emission computed tomography/computed tomography (SPECT/CT) fusion, add significantly to diagnostic confidence.

Department of Radiology, Nuclear Radiology Section, Boston Medical Center/Boston University School of Medicine, Boston, MA.

Address reprint requests to Tira Bunyaviroch, MD, Nassau Radiologic Group, PC, 990 Stewart Ave, Garden City, NY 11530. E-mail: tbunyaviroch@hotmail.com

Radiopharmaceuticals

The radiopharmaceuticals used to diagnose infection and inflammation can be categorized into infection/inflammation-seeking agents and other agents with patterns associated with infection/inflammation. The infection/inflammation-seeking agents widely used today are ^{67}Ga, indium-111 (^{111}In)-labeled WBCs, and ^{99m}Tc-labeled WBC. ^{99m}Tc diphosphonates (methylene diphosphonate [MDP] and hydroxymethylene diphosphonate [HDP]) are examples of radiotracers that have patterns associated with an infectious or inflammatory process and are often used in combination with the inflammation-seeking agents for increased specificity. Some examples include ^{99m}Tc-MDP bone scan with ^{67}Ga, or ^{111}In WBCs with ^{99m}Tc sulfur colloid bone marrow scan. Analogously, thallium-201 chloride (^{201}T1) has been successfully used in combination with ^{67}Ga for differentiating cerebral toxoplasmosis from lymphoma.[3]

New radiopharmaceuticals and new technologies demonstrate significant potential for the future of infection imaging. Ongoing research into radiolabeled monoclonal antibodies such as ^{99m}Tc fanolesomab demonstrate some advantages to standard agents, including ease of preparation and potentially better imaging characteristics.[4] Similarly, ^{99m}Tc ciprofloxacin has demonstrated potential for the localization of infections.[5–8] ^{18}F FDG-PET also has demonstrated value in imaging patients with suspected infection.[9,10]

^{67}Ga

^{67}Ga is a readily available radiopharmaceutical used in the localization of infectious and inflammatory processes. As an iron analog,[11] ^{67}Ga binds to

0001-2998/06/$-see front matter
doi:10.1053/j.semnuclmed.2006.05.004

Table 1 Radiopharmaceuticals

	^{67}Ga Citrate	^{111}In WBCs	^{99m}Tc WBCs
Physical properties	Cyclotron Produced $T_{1/2}$ = 78 h Photopeaks: 93, 185, 300, 394 keV	Cyclotron Produced $T_{1/2}$ = 67 h Photopeaks: 173, 247 keV	Generator Produced $T_{1/2}$ = 6 h Photopeak: 140 keV
Preparation	None	In vitro labeling: 60 cc of blood, isolation of WBCs, incubation with ^{111}In oxine	In vitro labeling: 60 cc of blood, isolation of WBCs, incubation with ^{99m}Tc HMPAO
Route of administration	IV	IV	IV
Dose (adult)	5.0-7.5 mCi	0.5 mCi	25 mCi
Biodistribution	Liver, skeleton, spleen, nose, salivary and lacrimal glands, breasts, genitalia	Spleen, liver, bone marrow	Spleen, liver, bone marrow, GU tract, GI tract
Mechanisms of localization	Hyperemia; increased capillary permeability; iron-binding proteins (transferrin, lactoferrin); siderophores	Migration of WBCs; chemotaxis	Migration of WBCs; chemotaxis
Routes of excretion	GU tract (1st 24 h); GI tract	None	GU tract (1st 4 h); GI tract (after 4 h)
Dosimetry	7 rad/5 mCi colon; 1 rad/5 mCi body	20 rad/0.5 mCi spleen; 0.5 rad/0.5 mCi body	15 rad/25 mCi colon; 1.5 rad/25 mCi body
Timing	48-72 h	18-24 h	2-4 h; 24 h (optional)
Instrumentation	Dual-detector gamma camera; medium-energy collimator; 3 photopeaks	Dual-detector gamma camera; medium-energy collimator; 2 photopeaks	Dual-detector gamma camera; low-energy collimator; 1 photopeak
Imaging protocols	Whole-body or regional planars; whole-body or regional SPECT		
Adjunctive imaging	Planar ± SPECT ^{99m}Tc MDP bone scan	Planar ± SPECT ^{99m}Tc sulfur colloid marrow scan	None
Advantages	No labeling	No GI or GU excretion	Optimal imaging characteristics; dose (children)
Limitations	Delayed imaging (GI tract activity)	IV access; leukopenic (WBC < 4,000); abnormal WBCs; dose (children)	IV access; leukopenic (WBC < 4,000); abnormal WBCs

transferrin,[12,13] lactoferrin,[14,15] and siderophores,[16] which allow it to diffuse through loose endothelial junctions of capillaries at sites of inflammation and enter the extracellular fluid space.[17] After leaking into areas of inflammation, ^{67}Ga is bound to iron-binding proteins of inflammatory cells, bacterial siderophores, or other mucopolysaccaride proteins.[18] Because ^{67}Ga binding does not rely solely on white blood cell migration, this agent is useful in the evaluation of leukopenic patients.[19]

Radiolabeled WBCs

^{111}In oxine was the first radiolabel found suitable for labeling WBCs.[20,21] To function as an infection/inflammation-seeking agent, ^{111}In oxine, as well as ^{99m}Tc hexamethylpropylene amine oxime (HMPAO), must be bound to WBCs. The process of radiolabeling WBCs must be performed in vitro because of the nonspecific labeling by the ^{111}In oxine and ^{99m}Tc HMPAO. A 60-mL sample of blood is required. WBCs must be separated from the red blood cells and platelets by differential centrifugation without damaging the WBCs. The WBCs are then resuspended and incubated with ^{111}In oxine or ^{99m}Tc HMPAO. After washing off the unbound radiolabel, the radiolabeled WBCs can be reinjected into the patient. Once reinjected into the patient, the localization of radiolabeled WBCs depends on intact chemotaxis, the number and types of cells labeled, and cellular component of the inflammatory response.[4] In addition, a total WBC count of at least 4000/mm^3 is needed to obtain diagnostic images. Neutrophils comprise the majority of radiolabeled leukocytes and therefore localize preferentially to neutrophil-mediated processes such as bacterial infections. Conversely, radiolabeled WBCs are less effective in nonneutrophilic processes, such as tuberculous infections.[22]

The ability to radiolabel WBCs with ^{99m}Tc HMPAO has allowed better image quality with larger doses and more favorable imaging characteristics. The physiologic distribution of ^{99m}Tc WBCs, however, is different from ^{111}In WBCs. The major difference is the presence of physiologic gastrointestinal and genitourinary activity that is absent in ^{111}In WBC studies. A comparison of abscess to normal soft-tissue radiotracer levels using ^{99m}Tc WBCs and ^{111}In WBCs demonstrated lower abscess concentrations using ^{99m}Tc WBCs.[23,24] In contrast, imaging comparisons have shown that ^{99m}Tc WBCs have equal or greater sensitivity than ^{111}In WBCs.[25,26] Given the different physiologic distributions, the choice of radiotracer will likely depend on the organ or region of interest and radiopharmaceutical availability.

Table 2 Preferred Indications for Infection/Inflammation-Seeking Agents

	^{67}Ga	^{111}In WBCs	^{99m}Tc WBCs
Occult sepsis	+/−	+	+/−
Abdominal abscess	−	+	−
Acute abscess	−	+	+/−
Chronic abscess	+	−	−
Pyogenic abscess	−	+	+
Nonpyogenic abscess	+	−	−
Inflammatory bowel disease	−	+	+ (children)
Renal abscess	−	+	−
Pulmonary Infection in HIV+	+	−	−
Nonpulmonary Infection in HIV+	−	+	+
Lymphadenitis in HIV+	+	−	−
Acute bone and joint infection	−	+	−
Chronic bone and joint infection	+	+/−	−
Complicated bone and joint infection	+/−	+	−
Infected bone and joint prosthesis	+/−	+	−
Spine/disc space infection	+	−	−
Infected catheters/vascular grafts	−	+	−
Pediatric infection/inflammation	+	−	+
Granulomatous disease (sarcoid)	+	−	−

Comparison of Infection/ Inflammation-Seeking Agents

Table 1 lists the properties, advantages, and limitations of ^{67}Ga and radiolabeled WBCs. In a practical sense, ^{67}Ga has an advantage by not requiring the sampling, labeling, and reinjection of blood products. ^{111}In and ^{99m}Tc WBCs do require handling and labeling of WBCs, which requires time, careful identification of the samples, and a minimum number of white cells. ^{111}In WBCs have a more favorable biodistribution, with an absence of gastrointestinal and genitourinary excretion. ^{99m}Tc WBCs have more favorable imaging characteristics and expose patients to lesser radiation doses.

Experimental evidence in dogs demonstrated greater abscess-to-blood ratios using ^{111}In WBCs versus ^{67}Ga, suggesting a potential advantage for infection detection.[27] In human testing, ^{111}In WBCs were shown to be an accurate method of detecting abdominal/pelvic abscesses with a sensitivity and specificity of 90% and 95%, respectively.[28] In comparison with ^{67}Ga, ^{111}In WBCs do not accumulate within the colon or healing, uninfected wounds. In addition, a prospective evaluation of 32 patients with suspected infection demonstrated false-negatives using ^{111}In WBCs with infections greater than 2 weeks old and using ^{67}Ga with infections of less than 1 week.[29] Table 2 lists the preferred indications for these infection/inflammation-seeking agents. Many early comparisons have been performed between ^{67}Ga and ^{111}In WBCs. Sfakianakis and coworkers performed a prospective study in 32 patients to evaluate these agents in the diagnosis of occult sepsis.[29] They found greater specificity and accuracy using ^{111}In WBCs (specificity 98%, accuracy 94%), versus ^{67}Ga (specificity 91%, accuracy 90%).

Imaging

Fusion Methodologies

In the 1970s, a potential improvement in the anatomic detail of nuclear imaging was investigated.[30,31] Emission computed tomography, as its name implies, created scintigraphic tomographic images whereas previously physicians were limited to planar images. Jaszczak and coworkers[30] studied 25 patients with intracranial lesions and determined that the average lesion contrast of SPECT was superior to planar scintigraphy by a factor greater than 2. In the same decade, others were investigating the benefits of CT.[32,33] The integration of these technologies has taken some time to develop after their initial development and introduction into routine diagnostic medical imaging.

The desire to integrate these tomographic imaging technologies was predicated on their distinct and complementary roles of functional and anatomic evaluation. The process of integrating SPECT and CT initially began with the side-by-side visual comparison of 2 imaging studies performed on a given patient. With this method, physicians needed to rely on their own spatial sense and mentally fuse the 2 image sets.[34] Today, this process is still performed commonly. However, the mental registration of images frequently is difficult because of differences in patient positioning and size differences between imaging studies. As computer technology improved, software fusion of SPECT and CT images became possible. Objective methods, such as software fusion, could enable more optimal diagnosis and treatment.[34] Similar difficulties in accurate image registration were encountered as the result of differences in patient positioning on examinations done at different times.

Extrinsic and intrinsic image-based software algorithms were designed to correct for these issues. Extrinsic methods used external fiducial markers during scintigraphy and radiography. For the evaluation of brain tumors, this method has a good degree of accuracy and the potential to improve specificity.[35] Intrinsic methods rely on anatomical or geometrical landmarks, image gray values, and the alignment of structures to register images.[36] Registration of images by the alignment of anatomic structures is referred to as the segmentation method and can either be rigid or flexible. Rigid segmentation techniques do not allow the individual image sets to be modified to accommodate altered positioning whereas flexible segmentation attempts to do just that.

Eventually, hardware fusion where SPECT and CT images are acquired on the same machine at the same time became available. As a tomographic imaging modality, positron emission tomography (PET) imaging followed the same progression toward fusion with CT. Hardware fusion attempts to remove a major difficulty in SPECT/CT fusion, namely the change in patient positioning between studies. Software fusion for the brain has met with general success. The reason is likely attributable to the immobility of most structures within the head. Software fusion of the remainder of the body has not been as successful because of the inability to control motion and positioning between studies.[37] Specifically, the retrospective process of software fusion cannot control for cardiac and respiratory motion, nor can it control for gastrointestinal peristalsis and patient motion. Hardware fusion promises to eliminate the drawbacks of software techniques by limiting motion and time delay between the acquisitions of separate modalities. Furthermore, as a prospective fusion process, hardware fusion allows for cardiac and respiratory gating which potentially eliminate misregistration caused by motion artifact.

Clinical Applications of Fusion

There are many examples in the literature demonstrating the utility of SPECT/CT fusion, mostly for the evaluation of tumors but a few for infection and inflammation (Table 3).[38-52] Undoubtedly, functional and anatomic fusion can have a significant impact on patient management. In one of the earlier studies, Swayne[38] performed a prospective evaluation of software SPECT and CT fusion, using a flexible fusion algorithm, in ten patients with suspected inflammatory disease. Correct localization was found in all 10 patients, suggesting an accurate method of functional and anatomic correlation. Several subsequent investigations have shown that SPECT/CT fusion is beneficial to interpretation in a majority of cases[45] and increases sensitivity and specificity.[43] For the fusion of rigid structures such as the brain, it is likely that a fusion method based on intrinsic structures within the image is

Table 3 SPECT/CT Fusion Literature

Study	Disease	Radiopharmaceuticals	Patients	Modalities	Fusion Method	Conclusions
Swayne 1992[38]	Infection	^{67}Ga, ^{111}In WBCs, ^{99m}Tc-MDP	10	SPECT + CT	Software	Correct localization in all 10 cases; facilitation of percutaneous or surgical procedures in 6 of 10 cases
Horger 2003[39]	Infection	^{99m}Tc-labeled antigranulocyte antibodies	27	Integrated SPECT/CT	Hardware	Improved specificity of SPECT/CT fusion versus SPECT alone from 78% to 89%
Bar-Shalom 2006[40]	Infection	^{67}Ga, ^{111}In WBCs	82	Integrated SPECT/CT	Hardware	Improved diagnosis, localization, and definition of extent of disease in 48% of patients using SPECT/CT fusion versus scintigraphy alone (planars + SPECT)
Utsunomiya 2005[41]	Tumor (bone metastases)	^{99m}Tc-MDP	45	Integrated SPECT/CT	Hardware	Improved diagnostic confidence using SPECT/CT fusion versus side-by-side correlation
Filippi 2006[42]	Tumor (brain tumors)	^{99m}Tc tetrofosmin	30	Integrated SPECT/CT	Hardware	Significant clinical impact in 43% of cases
Kramer 1989[43]	Tumor (colorectal adenocarcinoma)	^{111}In-labeled anticarcinoembryonic antigen (CEA)	8	SPECT + CT	Software	Increased specificity of SPECT and increased sensitivity of CT
Even-Sapir 2001[44]	Tumor (endocrine tumors)	^{111}In octreotide, ^{99m}Tc MIBI, ^{131}I, ^{123}I MIBG, ^{75}Se cholesterol	27	Integrated SPECT/CT	Hardware	Improved image interpretation in 41%; provided additional information of clinical value in 33%
Yamamoto 2003[45]	Tumor (thyroid cancer)	^{131}I	17	SPECT + CT	Software	Fusion beneficial to interpretation in 88% of patients
Ruf 2004[46]	Tumor (thyroid cancer)	^{131}I	25	Integrated SPECT/CT	Hardware	Improved anatomic localization in 44% of lesions
Pfannenberg 2003[47]	Tumor (neuroendocrine tumors)	^{111}In octreotide and ^{123}I MIBG	54	Integrated SPECT/CT	Hardware	Altered interpretation in 51% of cases; therapeutic changes in 28% of cases
Krausz 2003[48]	Tumor (neuroendocrine tumors)	^{111}In octreotide	72	Integrated SPECT/CT	Hardware	Affected diagnostic interpretation in 32% using SPECT/CT versus scintigraphy alone; changed management in 14%
Amthauer 2005[49]	Tumor (neuroendocrine tumors)	^{111}In octreotide	27	Integrated SPECT/CT + diagnostic CT	Hardware and Software	Software fusion with high-resolution CT more accurate (88%) than hardware fusion (76%) or side-by-side analysis (60%)
Profanter 2004[50]	Tumor (parathyroid adenoma)	^{99m}Tc MIBI	6	SPECT + CT	Software	Exactly predicted localization and dimensions of solitary adenomas in 5 out of 6 patients
Schillaci 2004[51]	Tumor (hepatic hemagioma)	^{99m}Tc RBCs	12	Integrated SPECT/CT	Hardware	Significant impact on interpretation in 33%; improved accuracy from 71% using SPECT alone to 88% with SPECT/CT
Schettino 2004[52]	Tumor (prostate cancer)	^{111}In capromab	67	SPECT + CT–MR	Software	Improved specificity of SPECT by fusion with MRI/CT

more reliable than the placement of external markers. Nevertheless, the intrinsic software fusion of these modalities provided very good registration.

Software image fusion in the remainder of the body has had variable results. The evaluation of software fusion is difficult and even more challenging for flexible segmentation methods.[53] Limitations in the proper alignment of nonhead imaging encouraged the development of integrated SPECT/CT (hardware fusion) to increase the accuracy of tumor localization, assessment of invasion, and characterization of functional status.[54] In multiple studies, SPECT/CT fusion has successfully resolved inconclusive findings on planar scintigraphy,[54] improved anatomic localization,[46] increased specificity,[39] increased diagnostic confidence,[41] changed the interpretation of studies[47,48] and resulted in therapeutic modifications.[47] The pitfalls of not performing image fusion are well-illustrated in a case presentation of an ictal brain SPECT. A suspected seizure focus on interictal and ictal brain SPECT fused to a region in the sphenoid sinus, representing sinusitis rather than a seizure focus.[55]

Little doubt exists that dual-modality image correlation increases the accuracy of both studies. Side-by-side correlation is the least computer intensive method; however, it is the most mentally challenging. There are benefits and limitations to both software and hardware fusion, and the choice of fusion method will likely depend not only on the availability of equipment, but the body part and suspected pathology to be imaged.

Summary of Fusion Imaging

The use of SPECT/CT image fusion has largely concentrated on oncologic and neurologic disease.[36,54,56] There are studies that have evaluated SPECT/CT for suspected infection and inflammation[38-40] (Table 3). Our experience with image fusion has involved multiple organ systems including the central nervous system, head and neck, chest, cardiovascular system, and abdomen. Case vignettes will be presented to illustrate the added benefit of SPECT/CT fusion for a variety of selected infections. The spectrum of cases provided will illustrate the versatility and applicability of SPECT/CT fusion in a multitude of body regions and disease processes.

Case Vignettes

Central Nervous System

Case 1

A patient with HIV presented with a low-density lesion in the right parietal lobe on brain CT (Fig. 1A). Toxoplasma infection and central nervous system lymphoma were suspected. ^{201}T1 SPECT/CT (Fig. 1B) demonstrated no abnormal uptake within this lesion. ^{67}Ga SPECT/CT (Fig. 1C) shows focal uptake corresponding to this lesion. SPECT/CT fusion aided in the precise localization of this lesion and added further confidence that the study was negative on ^{201}T1 and positive on ^{67}Ga, which is consistent with infection and not tumor. In our experience, SPECT/CT fusion significantly increases sensitivity and specificity for the detection of intracranial lesions and is particularly helpful in lesions of smaller size and deeper location.

Head and Neck

Case 2

A 23-year-old patient with a history of a right mandible odontogenic cyst resection and bone graft reconstruction presented with swelling and drainage from the right jaw. The initial evaluation was performed with ^{111}In WBC SPECT (Fig. 2A), showing accumulation of activity on the right. It is uncertain whether this represented a soft tissue or bony process. SPECT/CT (Fig. 2B) clearly demonstrates focal WBC accumulation in the right mandible (at the surgical site), indicating a bone graft infection. Only when SPECT images were fused with the preoperative CT could bone activity be discriminated from soft tissue activity. In this instance, SPECT/CT fusion was important for accurate anatomic localization to the mandibular bone at the site of bone grafting.

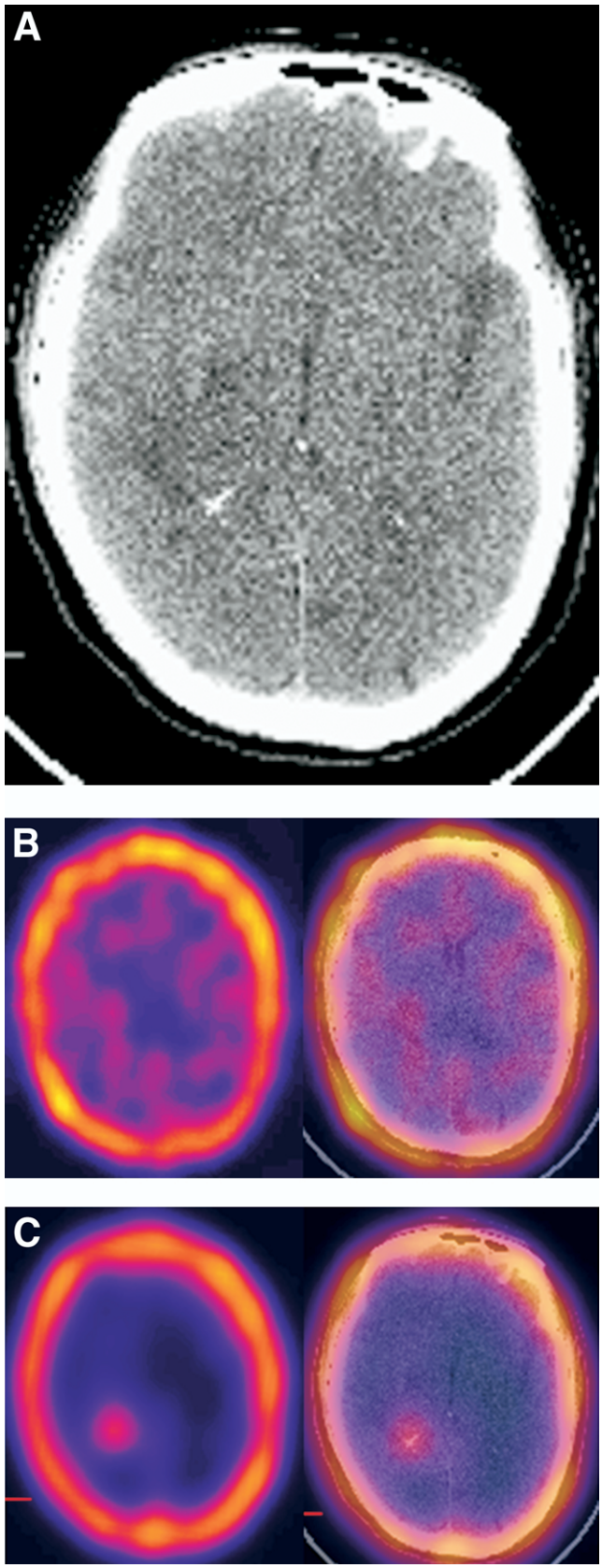

Figure 1 Nonspecific small low-density lesion in right parietal lobe on axial brain CT (A). ^{201}T1 SPECT and ^{201}T1 SPECT/CT (B) demonstrate no abnormal uptake. ^{67}Ga SPECT and ^{67}Ga SPECT/CT (C) show focal uptake in brain corresponding exactly to the CT lesion, indicating a brain abscess.

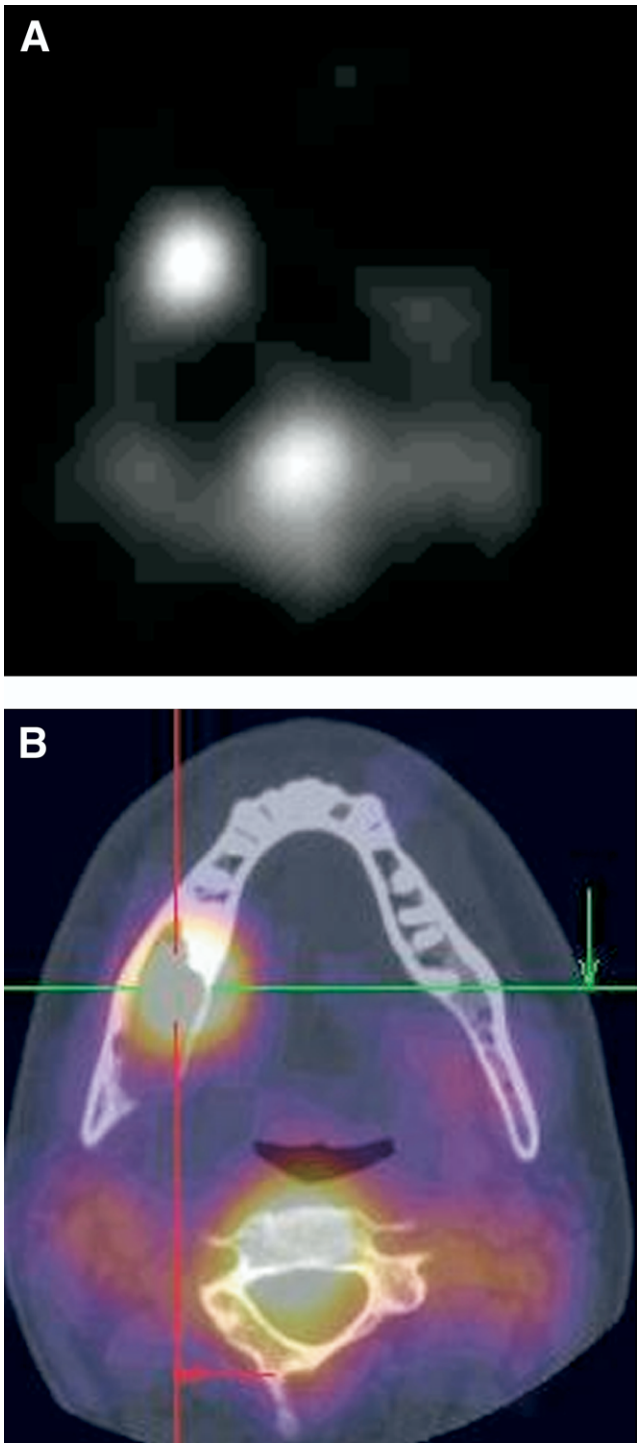

Figure 2 Axial ^{111}In WBC SPECT (A) and SPECT/CT (B) show focal WBC localization in the right mandibular bone (at the surgical site), indicating osseous infection.

Chest

Case 3

A ^{67}Ga scan was performed on a patient with HIV and chronic lymphocytic leukemia who presented with a persistent pneumonia. The ^{67}Ga whole-body planar (Fig. 3A) and SPECT (Fig. 3B) images demonstrate multifocal activity in the chest, abdomen, and pelvis. These lesions could not be further localized using SPECT alone (Fig. 3B) or side-by-side comparison with CT (Fig. 3C). SPECT/CT (Fig. 3D) confidently excluded infection in the abdomen and pelvis and localized the abnormal activity in the chest to the pneumonia (presumed *Pneumocystis carinii* pneumonia in this patient with HIV). The abnormal localization in the abdomen and pelvis correlated to physiologic bowel activity and adenopathy related to the patient's chronic lymphocytic leukemia. This case demonstrates the use of fusion to exclude relevant disease, thereby increasing the specificity of scintigraphy.

Case 4

A 56-year-old man with a history of advanced pulmonary sarcoidosis presents for the evaluation of cardiac sarcoid. The ^{67}Ga whole-body planar images (Fig. 4A) show low-grade gallium activity in chest. It is not clear on ^{67}Ga SPECT (Fig. 4B) whether the extensive bilateral disease in the chest involves the heart. The axial CT image (Fig. 4C) shows the patient's known bilateral pulmonary fibrosis, although morphologic abnormalities of the heart were difficult to discern. The addition of SPECT/CT (Fig. 4D) excluded involvement of the heart and localized the activity in the chest to the patient's bilateral pulmonary fibrosis. In this instance, SPECT/CT was crucial in the exclusion of cardiac disease because of the limited anatomic resolution of ^{67}Ga SPECT alone and the lack of morphologic changes on CT.

Case 5

The patient presents with sepsis and a history of a recent sternotomy and coronary bypass surgery. The clinical examination of the sternum and CT (Fig. 5A) were unremarkable. ^{111}In WBC SPECT/CT (Fig. 5B) and ^{99m}Tc sulfur colloid (bone marrow) SPECT/CT (Fig. 5C) were performed. Each scintigraphic study demonstrates linear activity in the sternum. Although the comparison of ^{111}In WBC and bone marrow scans suggest concordant radiotracer localization and a lack of infection, SPECT/CT demonstrated an anatomic discordance. ^{111}In WBC SPECT/CT (Fig. 5B) activity localizes to the mid sternum whereas bone marrow SPECT/CT (Fig. 5C) localizes to the right inferior sternum. Sternal osteomyelitis of the mid sternum was proven at surgery. Therefore, SPECT/CT demonstrated discordant activity that would otherwise have appeared concordant based on scintigraphic imaging alone.

Cardiovascular

Case 6

An 80-year-old patient presented with methicillin-resistant *Staphylococcus aureus* bacteremia that was unresponsive to vancomycin. ^{111}In WBC planar (Fig. 6A) and SPECT (Fig. 6B) imaging demonstrated nonspecific activity in the left chest that could not be further localized. CT (Fig. 6C) did not have a discernable anatomic abnormality to correspond with the scintigraphic findings. SPECT/CT (Fig. 6D) accurately localized the scintigraphic finding to the mitral valve, indicating a valvular infection. In this instance, the scintigraphic findings could not be resolved on planar imaging, SPECT imaging, nor side-by-side correlation. Fusion was necessary in this case for the accurate localization of the patient's disease.

Case 7

A 79-year-old patient presented with bacteremia and fevers and a history of CABG 8 years previously. ^{111}In WBC planar (Fig. 7A) and axial SPECT (Fig. 7B) imaging demonstrated focal activity in the left chest. The CT was without significant abnormality. SPECT/CT (Fig. 7C) localizes the activity to a subtle fluid collection in the pericardium, indicating a pericardial abscess. The fusion process increased the sensitivity of the CT and increased the specificity of the SPECT by localizing scintigraphic disease with subtle anatomic abnormality.

Case 8

A 72-year-old woman presented with sepsis after undergoing multiple procedures for her thoracoabdominal aortic aneurysm. Her disease course was complicated by an aortoduodenal fistula and the development of a hematoma around the aortic graft. CT of the chest (Fig. 8A) and abdomen (Fig. 8B) demonstrated postoperative changes and fluid around the thoracoabdominal aortic graft. These findings are nonspecific for infection. ^{111}In WBC planar imaging (Fig. 8C) demonstrated focal activity in the left upper quadrant. SPECT/CT of the chest (Fig. 8D) excluded tracer localization in the aortic graft. SPECT/CT of the abdomen (Fig. 8E) accurately localized the activity in the left abdomen within the abdominal aortic graft, indicating a

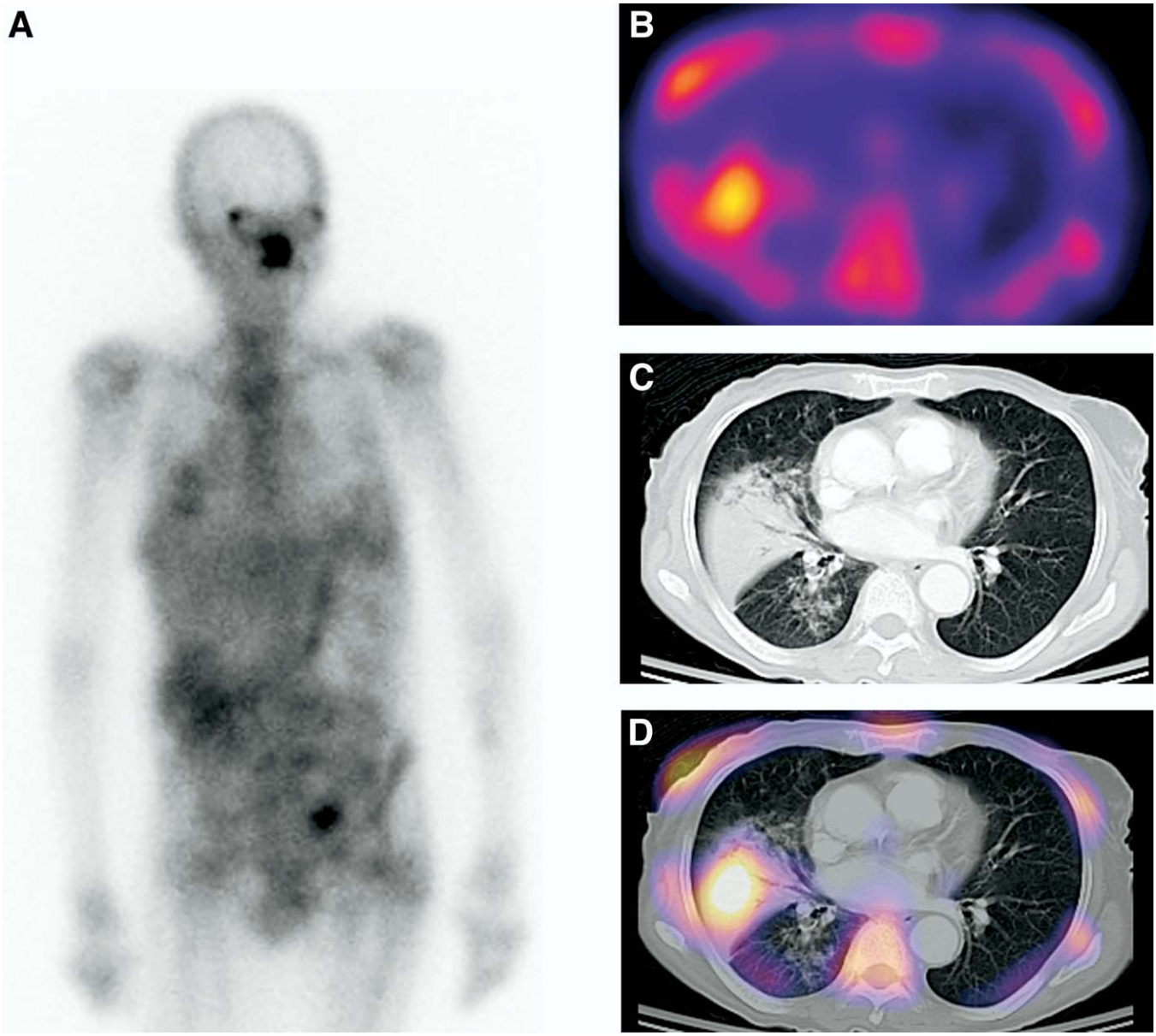

Figure 3 ^{67}Ga whole-body planar image (A) demonstrates nonspecific multifocal uptake in chest, abdomen and pelvis. Axial SPECT (B), CT (C), and SPECT/CT (D) localize the focal uptake to the right middle lobe pneumonia. The other abnormal sites corresponded to bowel and known adenopathy.

graft infection. Fusion added specificity to the widespread aortic abnormality seen on CT in addition to precisely localizing the scintigraphic abnormality.

Abdomen

Case 9

A 73-year-old man presented with bacteremia and a fever of unknown origin along with a prior history of endocarditis and prior vascular graft. ^{111}In WBC planar (Fig. 9A) and coronal SPECT (Fig. 9B) showed abnormal activity in the abdomen and pelvis that appeared patchy and noncontiguous. After fusion with CT (Fig. 9C), SPECT/CT (Fig. 9D) accurately demonstrated that all foci of activity conformed to the colon, indicating an active colitis. Subsequent stool analysis confirmed *Clostridium difficile* colitis. An infectious process of the aorta and vascular graft also was excluded. Fusion resolved the multiple foci of abnormal activity throughout the abdomen and excluded suspected sites of disease.

Case 10

A patient presented with a fever of unknown origin and a history of chronic lymphocytic leukemia. ^{67}Ga planar (Fig. 10A) and SPECT (Fig. 10B) imaging demonstrated suspicious focal activity in the right lower quadrant of the abdomen and hepatosplenomegaly. After fusion with CT (Fig. 10C), SPECT/CT (Fig. 10D) accurately localized the right lower quadrant activity to a normal cecum, indicating normal physiologic bowel activity. Delayed ^{67}Ga imaging several days later demonstrated clearance of cecal activity and confirmed the lack of disease. In this instance, fusion was able to exclude disease through the accurate localization of scintigraphic findings and facilitate a more rapid diagnosis.

Case 11

A 62-year-old woman presented with a fever of unknown origin and a prior rectosigmoid cancer resection complicated by a presacral abscess 2 years previously. The CT demonstrated soft tissue thickening in the presacral region which was suspicious for a recurrent presacral infection. ^{111}In WBC

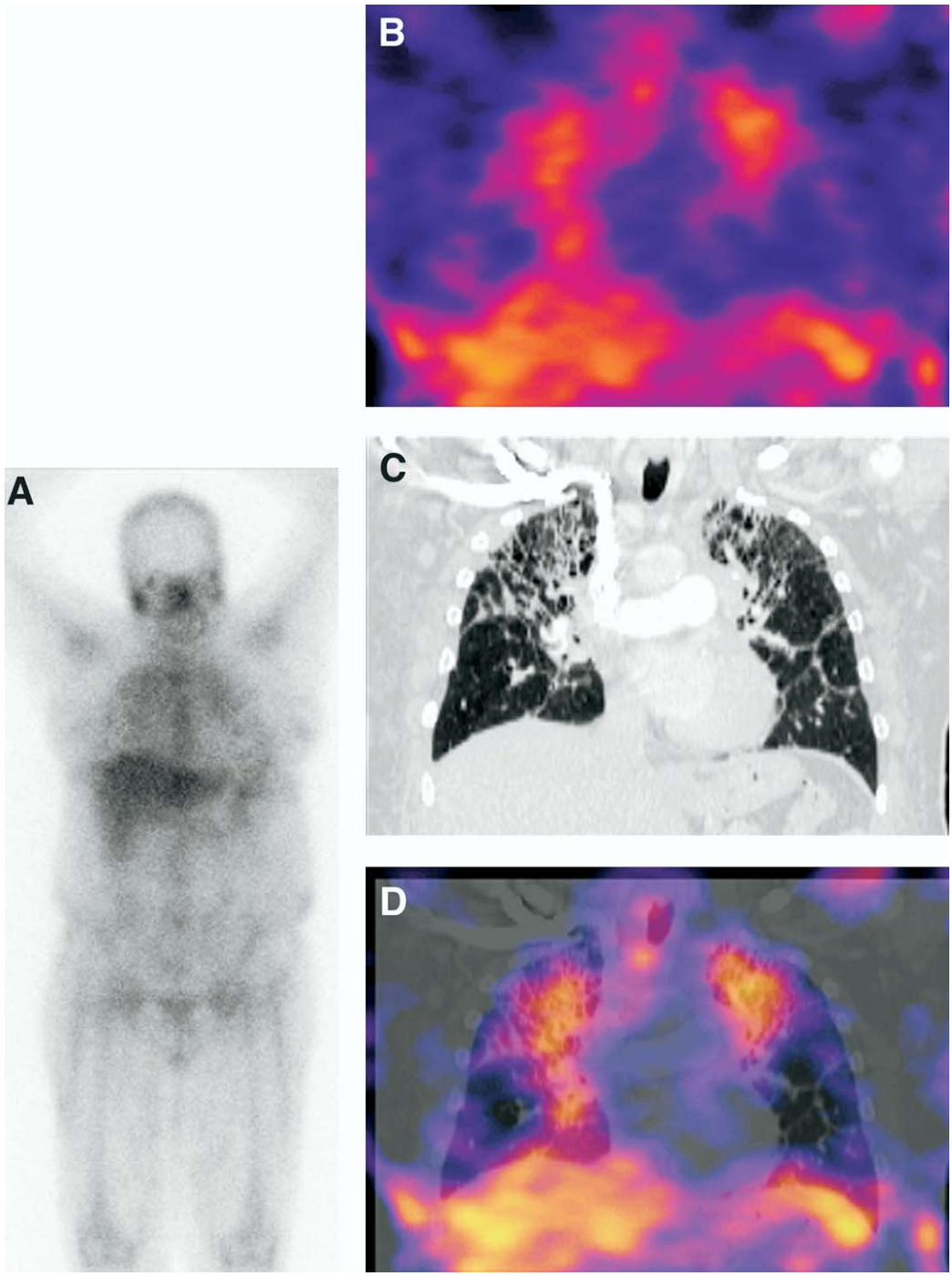

Figure 4 Extensive low-grade ^{67}Ga uptake in chest on planar (A) and coronal SPECT (B). Coronal CT (C) shows extensive pulmonary fibrosis. On coronal SPECT/CT (D), all abnormal activity localizes to pulmonary fibrosis, excluding cardiac involvement.

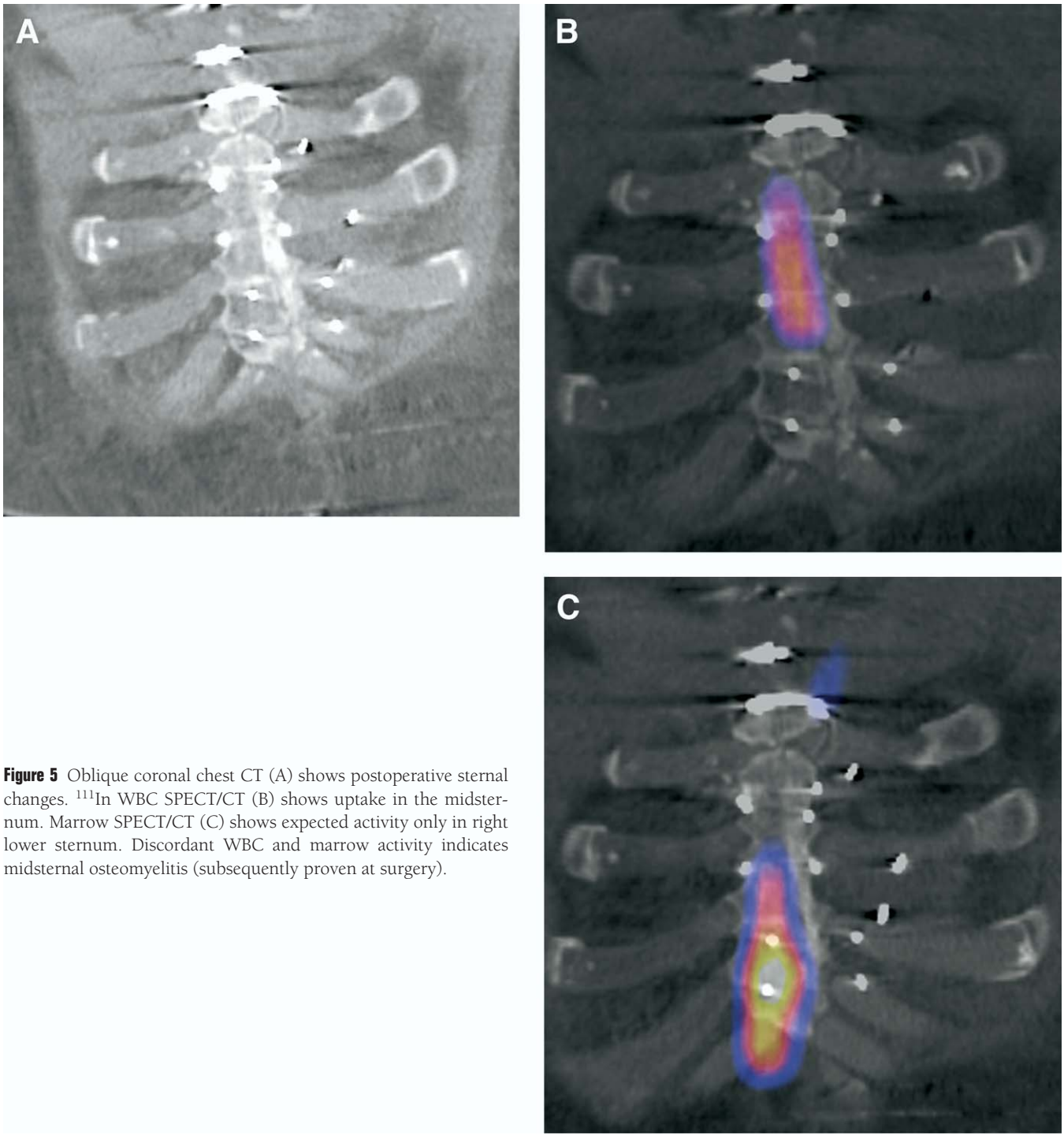

Figure 5 Oblique coronal chest CT (A) shows postoperative sternal changes. ^{111}In WBC SPECT/CT (B) shows uptake in the midsternum. Marrow SPECT/CT (C) shows expected activity only in right lower sternum. Discordant WBC and marrow activity indicates midsternal osteomyelitis (subsequently proven at surgery).

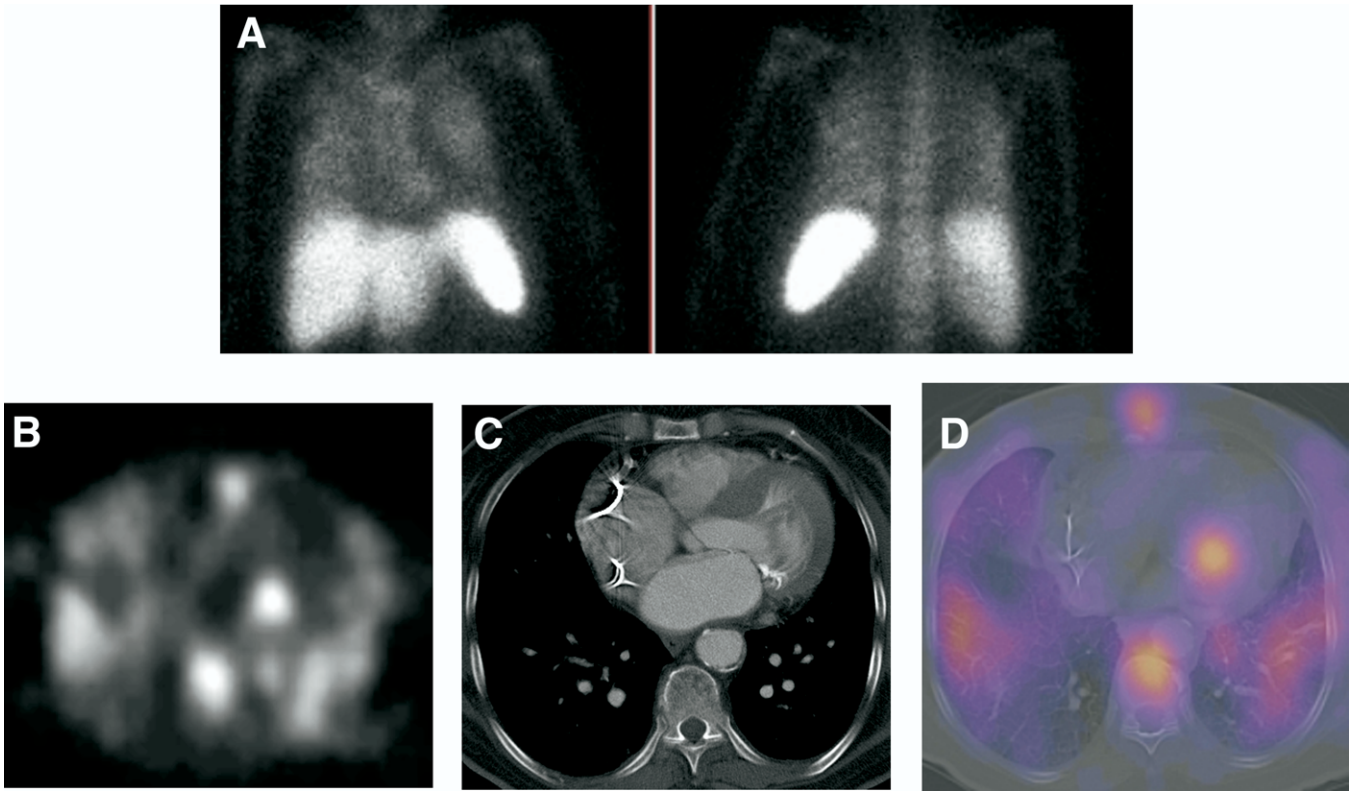

Figure 6 ^{111}In WBC planar (A) and axial SPECT (B) show abnormal focus of uptake in left chest. CT chest (C) shows mitral valve calcifications. SPECT/CT (D) localizes focus to mitral valve, indicating valvular infection.

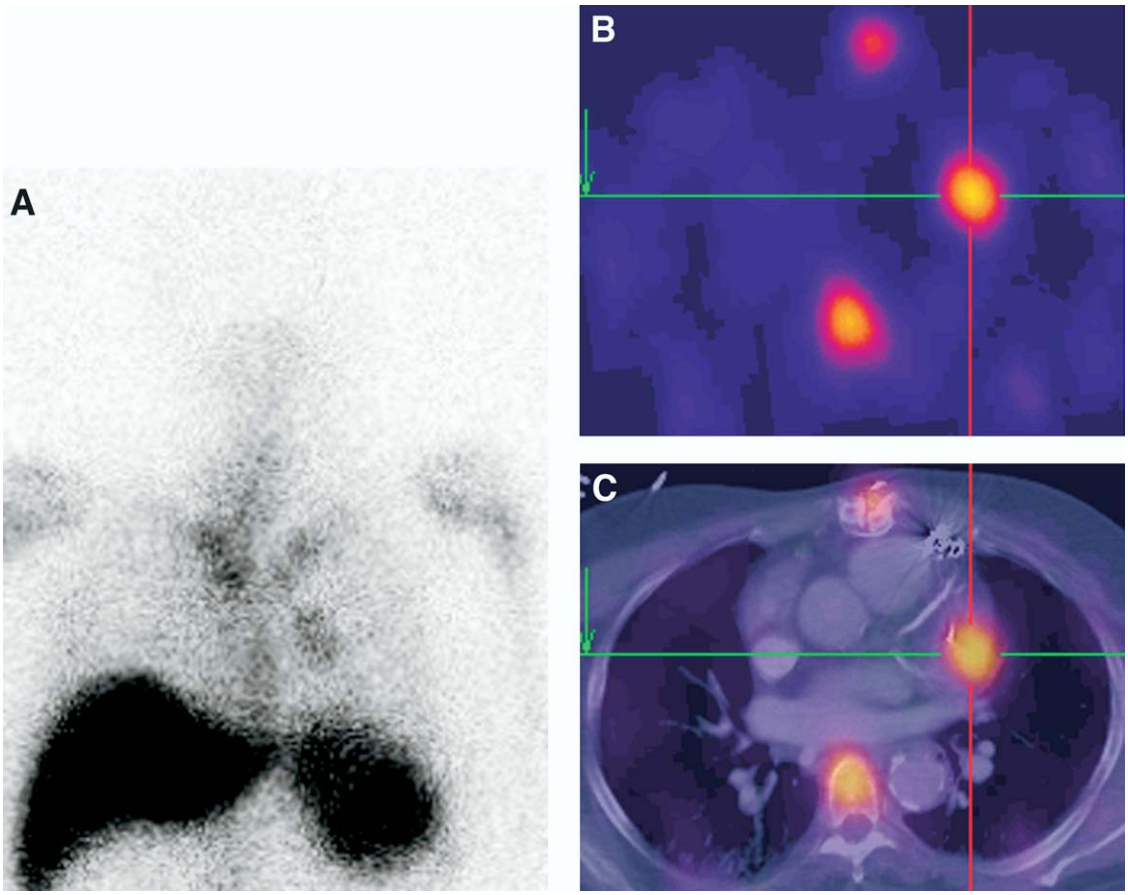

Figure 7 ^{111}In WBC planar (A) and axial SPECT (B) show intense focal uptake in left chest. SPECT/CT (C) accurately localizes the focus to left pericardium, indicating pericardial abscess.

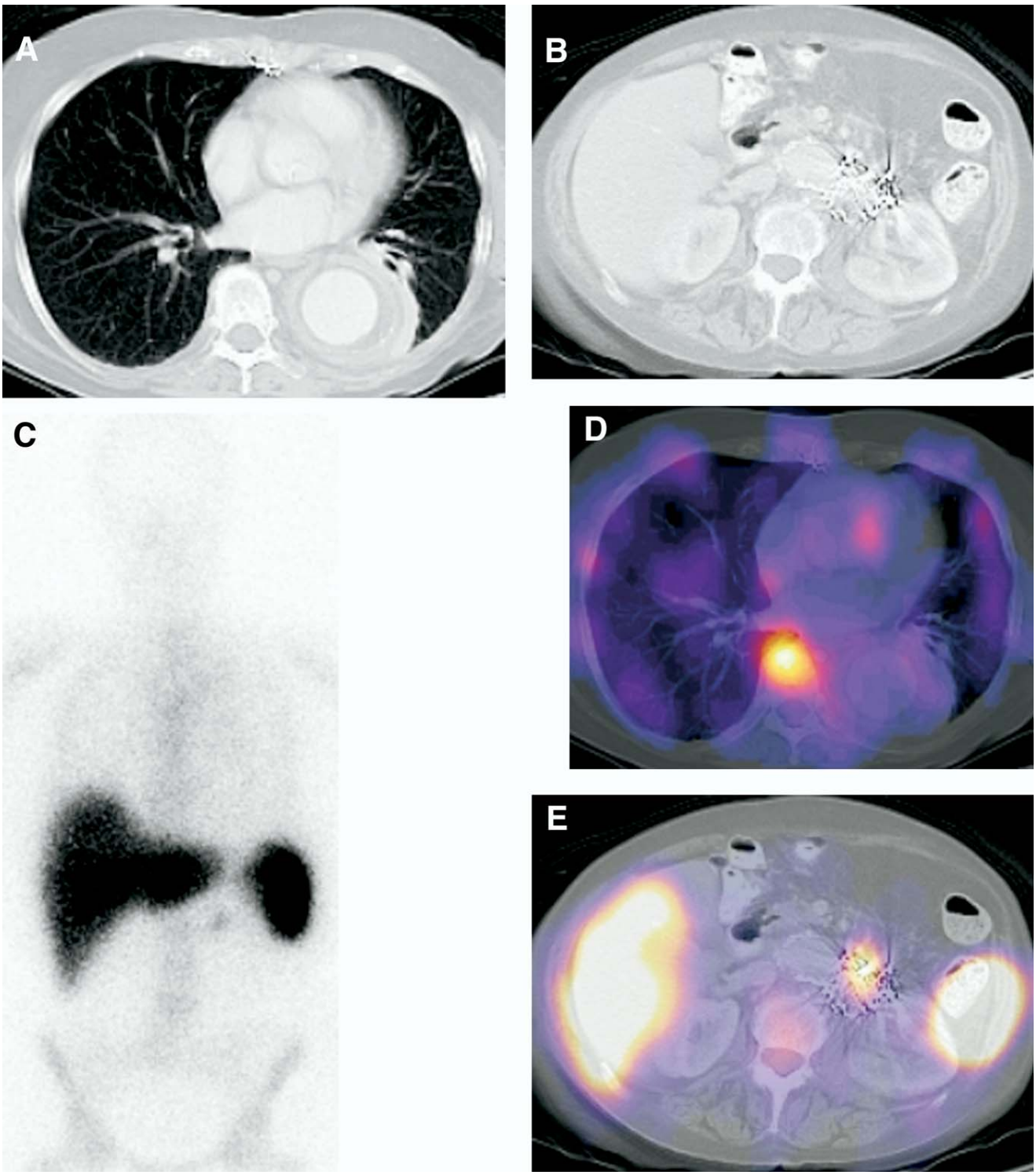

Figure 8 Thoracic CT (A) and abdominal CT (B) demonstrate perigraft fluid and postoperative changes. ^{111}In WBC planar (C) shows abnormal focus in left upper quadrant. No abnormal WBC localization in thoracic graft on axial SPECT/CT (D), but abnormal activity in abdominal aortic graft on axial SPECT/CT (E).

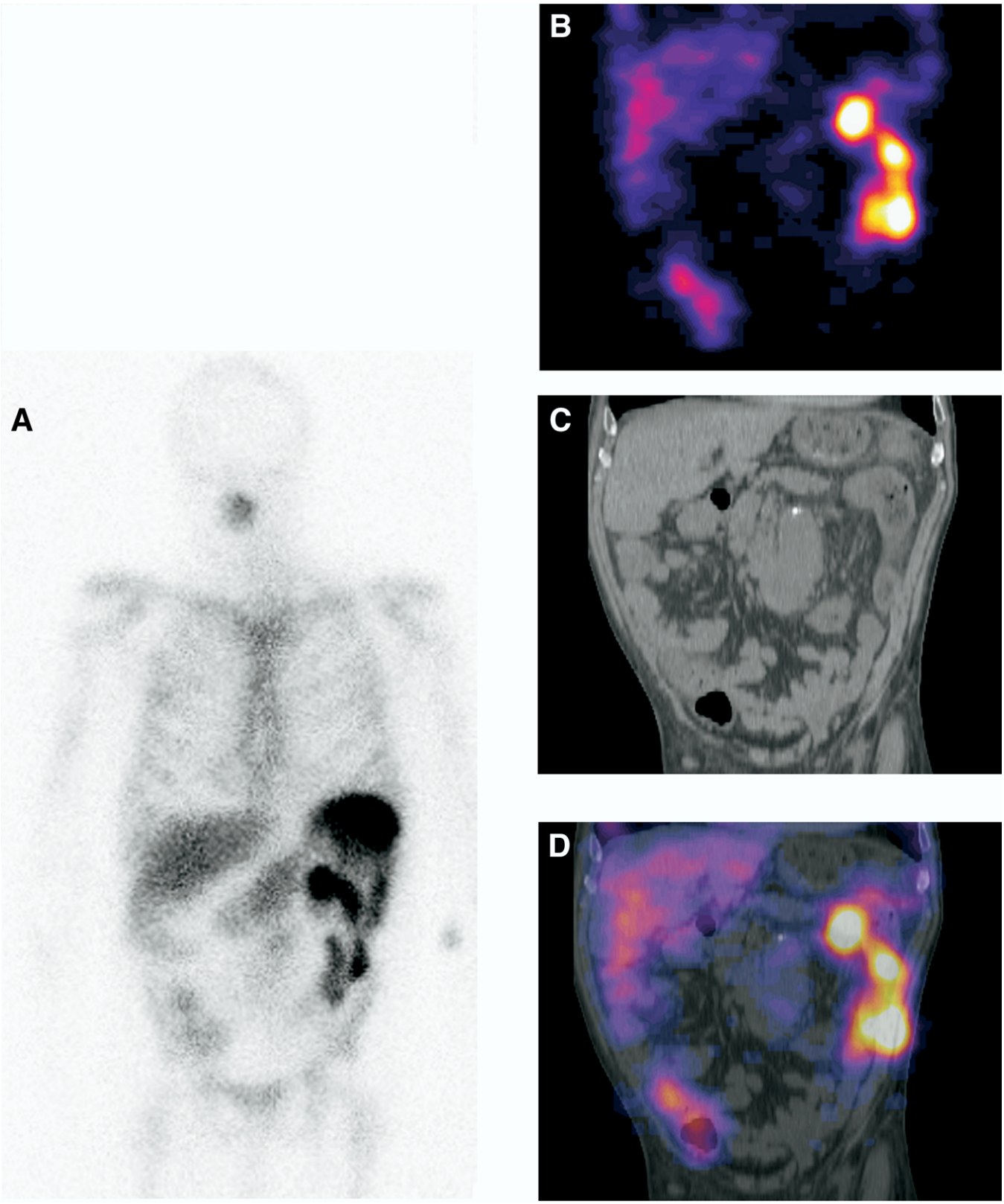

Figure 9 ^{111}In WBC planar (A) and coronal SPECT (B) show multifocal activity in abdomen and pelvis. Abdominal CT (C) and coronal SPECT/CT (D) accurately localize all abnormal activity to colon (*C. difficile* colitis), not vascular graft infection.

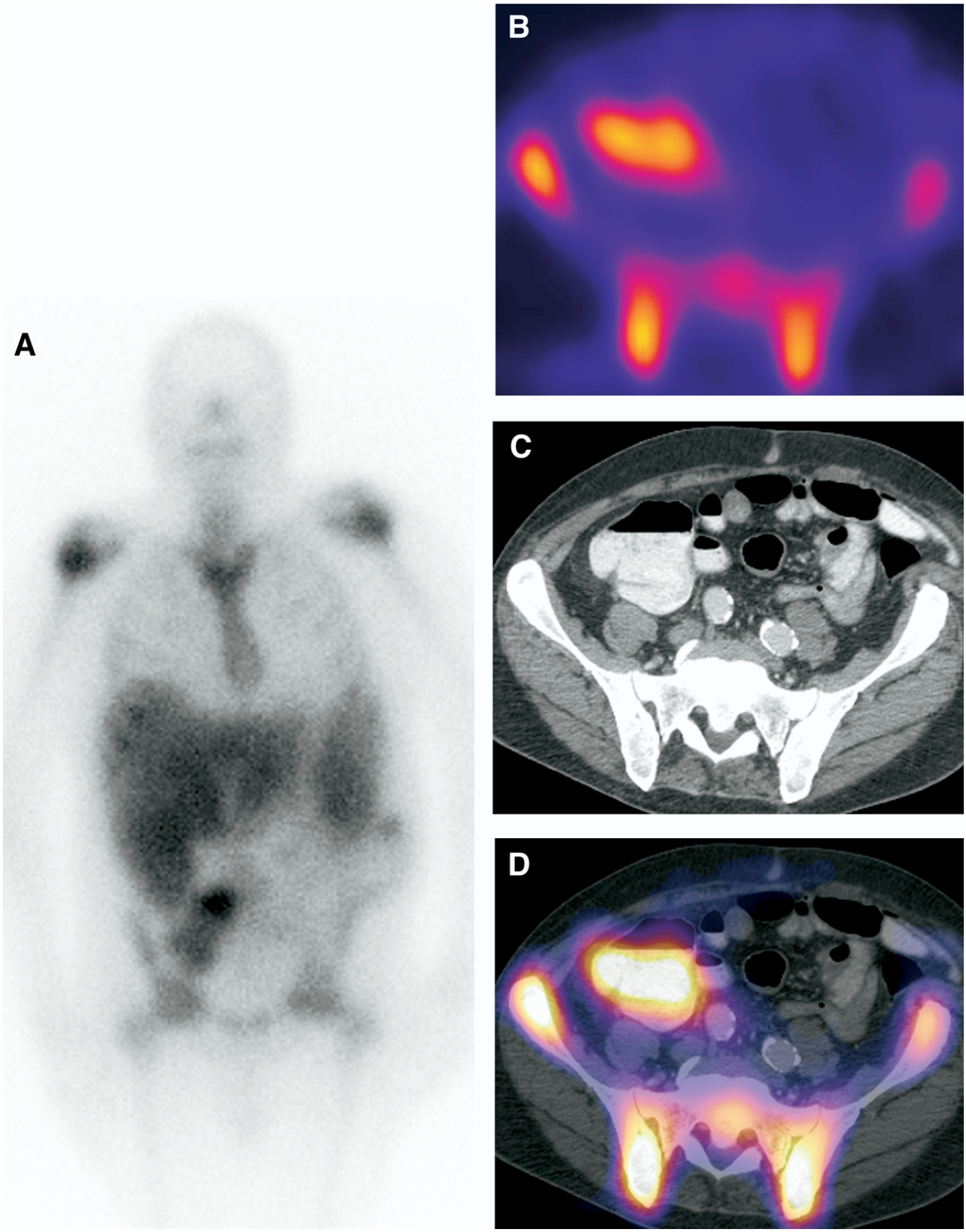

Figure 10 ^{67}Ga planar (A) and SPECT (B) show hepatosplenomegaly and suspicious nonspecific focal activity in right lower quadrant. Abdominal axial CT (C) and axial SPECT/CT (D) localize activity to cecum, likely physiologic.

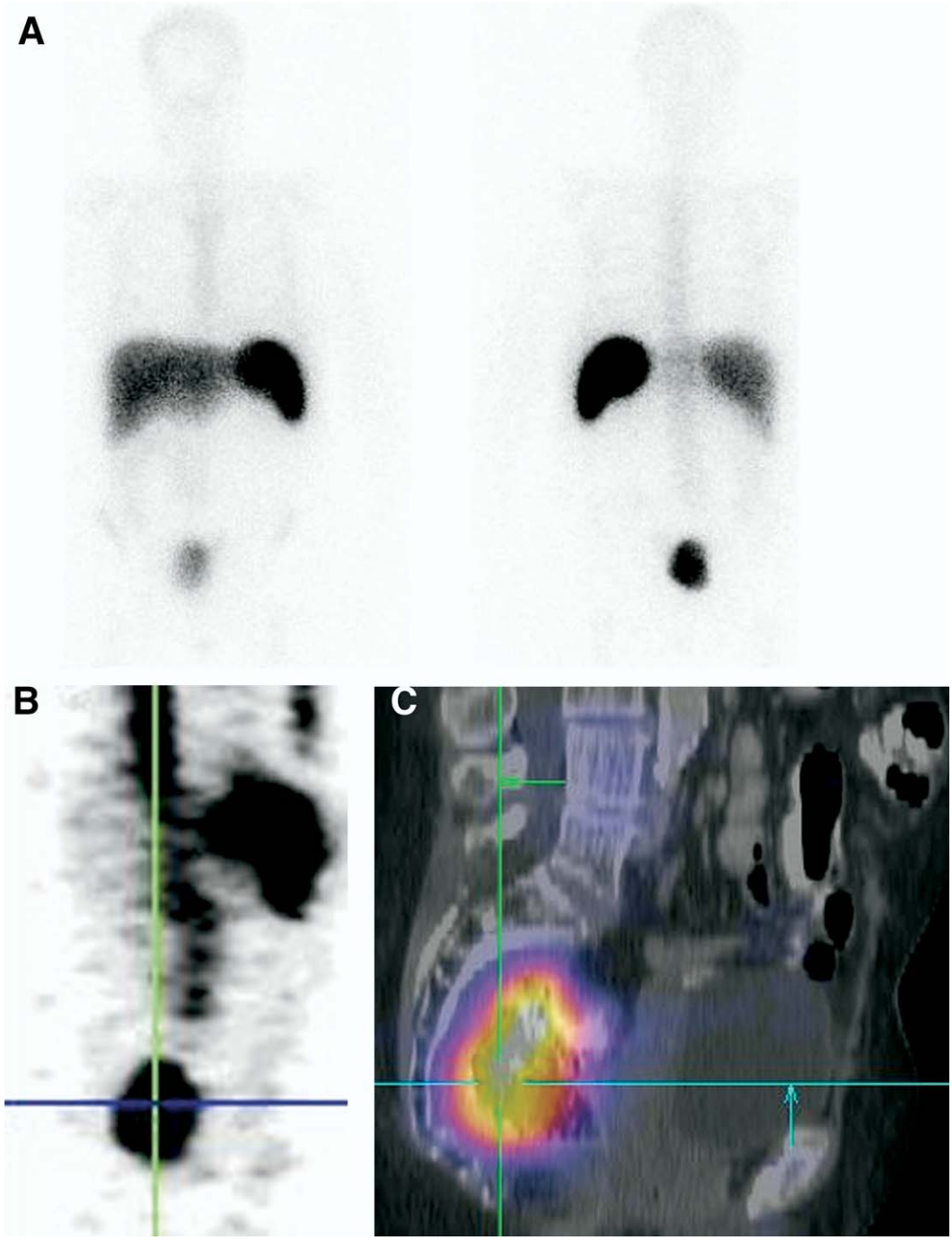

Figure 11 ^{111}In WBC planar (A) and SPECT (B) demonstrate focal intense uptake in pelvis. Sagittal SPECT/CT (C) localizes uptake to rectum (proctitis), not presacral soft tissues.

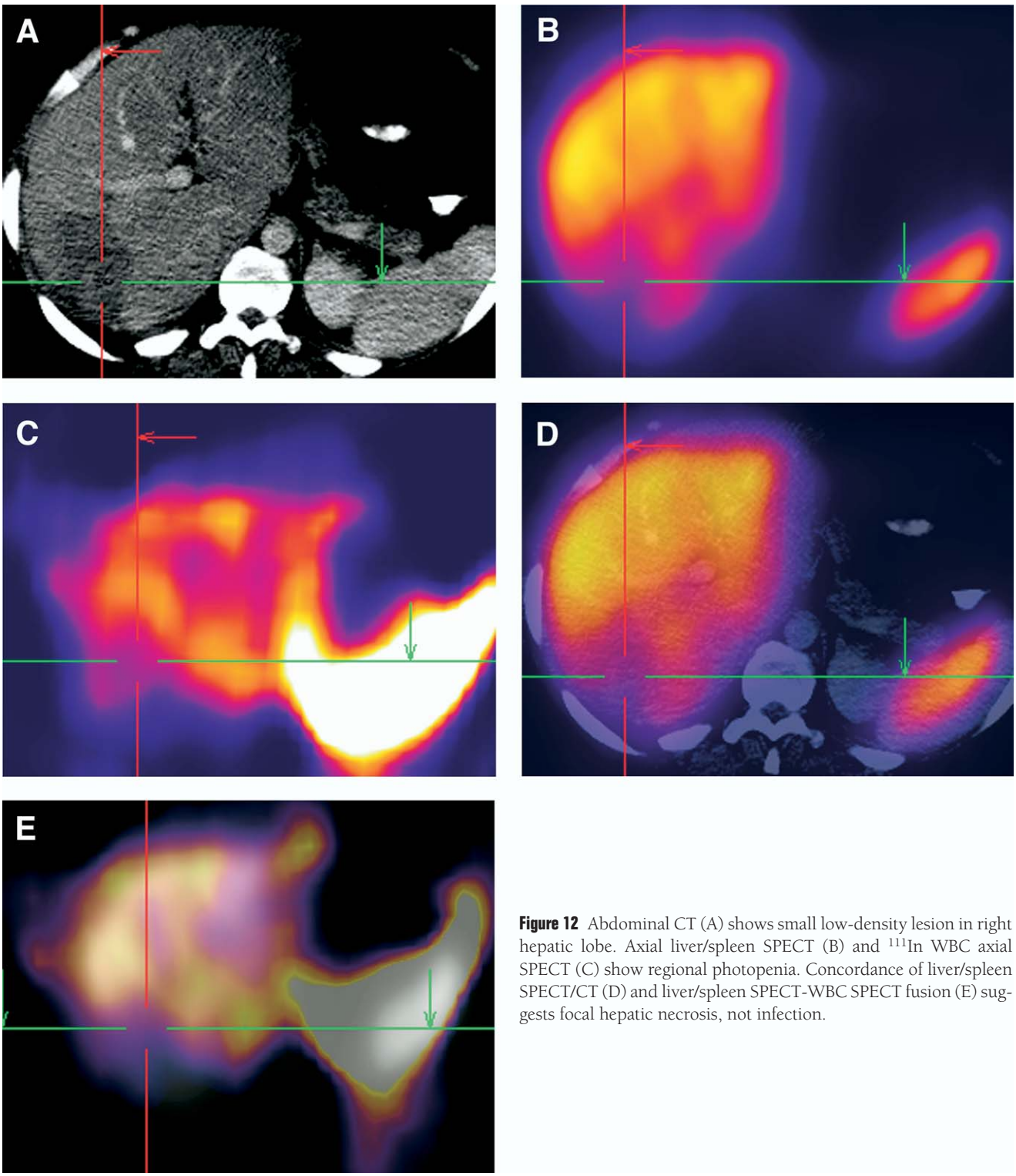

Figure 12 Abdominal CT (A) shows small low-density lesion in right hepatic lobe. Axial liver/spleen SPECT (B) and ^{111}In WBC axial SPECT (C) show regional photopenia. Concordance of liver/spleen SPECT/CT (D) and liver/spleen SPECT-WBC SPECT fusion (E) suggests focal hepatic necrosis, not infection.

planar (Fig. 11A) and SPECT (Fig. 11B) imaging demonstrate intense focal activity in the posterior pelvis. Side-by-side correlation suggested a presacral abscess. SPECT/CT (Fig. 11C) instead localized the activity to the rectum, thereby changing the diagnosis and excluding a recurrent presacral abscess. Colonoscopy with biopsy confirmed proctitis. Fusion thereby increased the specificity of the SPECT and CT and prevented a potential false-positive finding.

Case 12

A 30-year-old patient presented with fevers after a severe motor vehicle crash, liver lacerations, and a prolonged intensive care unit course. The CT (Fig. 12A) demonstrated a low-attenuation lesion in the right lobe of the liver, suspicious for infection, focal fatty infiltration, or infarction. A liver/spleen SPECT (Fig. 12B) and ^{111}In WBC SPECT (Fig. 12C) were performed, both demonstrating heterogeneous activity in the liver with ill-defined defects in the right lobe of the liver. SPECT/CT fusion of the liver/spleen scan (Fig. 12D) and ^{111}In WBC SPECT and liver/spleen SPECT fusion (Fig. 12E) demonstrated exact correlation of the ill-defined liver lesions with the focal defect on CT. The photopenic lesion on ^{111}In WBC and liver/spleen scan excluded infection and fatty infiltration and suggested a liver infarction. The use of fusion in this case improved anatomic localization and increased diagnostic confidence of the correct diagnosis.

References

1. McCall MS, Sutherland DA, Eisentraut AM, et al: The tagging of leukemic leukocytes with radioactive chromium and measurement of the in vivo cell survival. J Lab Clin Med 45:717-724, 1955
2. Athens JW, Mauer AM, Ashenbrucker H, et al: Leukokinetic studies. I. A method for labeling leukocytes with diisopropyl-fluorophosphate (DFP32). Blood 14:303-333, 1959
3. Lee VW, Antonacci V, Tilak S, et al: Intracranial mass lesions: sequential thallium and gallium scintigraphy in patients with AIDS. Radiology 211:507-512, 1999
4. Love C, Palestro CJ: Radionuclide imaging of infection. J Nucl Med Technol 32:47-57, 2004
5. Artiko V, Davidovic B, Nikolic N, et al: Detection of gastrointestinal and abdominal infections by ^{99m}Tc-ciprofloxacin. Hepatogastroenterology 52:491-495, 2005
6. De Winter F, Gemmel F, Van Laere K, et al: ^{99m}Tc-ciprofloxacin planar and tomographic imaging for the diagnosis of infection in the postoperative spine: experience in 48 patients. Eur J Nucl Med Mol Imaging 31:233-239, 2004
7. Gemmel F, De Winter F, Van Laere K, et al: ^{99m}Tc ciprofloxacin imaging for the diagnosis of infection in the postoperative spine. Nucl Med Commun 25:277-283, 2004
8. Yapar Z, Kibar M, Yapar AF, et al: The efficacy of technetium-^{99m} ciprofloxacin (Infecton) imaging in suspected orthopaedic infection: a comparison with sequential bone/gallium imaging. Eur J Nucl Med 28:822-830, 2001
9. Bleeker-Rovers CP, Vos FJ, Wanten GJ, et al: 18F-FDG PET in detecting metastatic infectious disease. J Nucl Med 46:2014-2019, 2005
10. Love C, Tomas MB, Tronco GG, et al: FDG PET of infection and inflammation. Radiographics 25:1357-1368, 2005
11. Hoffer P: Gallium: mechanisms. J Nucl Med 21:282-285, 1980
12. Hara T: On the binding of gallium to transferrin. Int J Nucl Med Biol 1:152-154, 1974
13. Aulbert E, Gebhardt A, Schulz E, et al: Mechanism of 67Ga accumulation in normal rat liver lysosomes. Nuklearmedizin 15:185-194, 1976
14. Hoffer PB, Huberty J, Khayam-Bashi H: The association of Ga-67 and lactoferrin. J Nucl Med 18:713-717, 1977
15. Weiner R, Hoffer PB, Thakur ML: Lactoferrin: its role as a Ga-67-binding protein in polymorphonuclear leukocytes. J Nucl Med 22:32-37, 1981
16. Muller G, Raymond KN: Specificity and mechanism of ferrioxamine-mediated iron transport in Streptomyces pilosus. J Bacteriol 160:304-312, 1984
17. Tsan MF: Mechanism of gallium-67 accumulation in inflammatory lesions. J Nucl Med 26:88-92, 1985
18. Newman RD, McAfee JG: Gallium-67 imaging in infection, in Sandler MP, Coleman RE, Patton JA, et al (eds): Diagnostic Nuclear Medicine (ed 4). Philadelphia, Lippincott, Williams, and Wilkins, 2004, pp 1205-1217
19. Dhawan VM, Sziklas JJ, Spencer RP: Localization of Ga-67 in inflammations in the absence of circulating polymorphonuclear leukocytes. J Nucl Med 19:292-294, 1978
20. McAfee JG, Thakur ML: Survey of radioactive agents for in vitro labeling of phagocytic leukocytes.I. Soluble agents J Nucl Med 17:480-487, 1976
21. McAfee JG, Thakur ML: Survey of radioactive agents for in vitro labeling of phagocytic leukocytes. II. Particles J Nucl Med 17:488-492, 1976
22. Palestro CJ, Torres MA: Radionuclide imaging of nonosseous infection. Q J Nucl Med 43:46-60, 1999
23. McAfee JG, Subramanian G, Gagne G, et al: ^{99m}Tc-HM-PAO for leukocyte labeling—experimental comparison with 111In oxine in dogs. Eur J Nucl Med 13:353-357, 1987
24. Mock BH, Schauwecker DS, English D, et al: In vivo kinetics of canine leukocytes labeled with technetium-^{99m} HM-PAO and indium-111 tropolonate. J Nucl Med 29:1246-1251, 1988
25. Peters AM, Roddie ME, Danpure HJ, et al: 99Tcm-HMPAO labelled leucocytes: comparison with 111In-tropolonate labelled granulocytes. Nucl Med Commun 9:449-463, 1988
26. Mountford PJ, Kettle AG, O'Doherty MJ, et al: Comparison of technetium-^{99m}-HM-PAO leukocytes with indium-111-oxine leukocytes for localizing intraabdominal sepsis. J Nucl Med 31:311-315, 1990
27. Thakur ML, Coleman RE, Welch MJ: Indium-111-labeled leukocytes for the localization of abscesses: preparation, analysis, tissue distribution, and comparison with gallium-67 citrate in dogs. J Lab Clin Med 89:217-228, 1977
28. Coleman RE, Datz FL: Detection of inflammatory disease with radiolabeled cells. in Sandler MP, Coleman RE, Patton JA, et al (eds): Diagnostic Nuclear Medicine (ed 4). Philadelphia, Lippincott, Williams, and Wilkins, 2004, pp 1219-1234
29. Sfakianakis GN, Al-Sheikh W, Heal A, et al: Comparisons of scintigraphy with In-111 leukocytes and Ga-67 in the diagnosis of occult sepsis. J Nucl Med 23:618-626, 1982
30. Jaszczak RJ, Murphy PH, Huard D, et al: Radionuclide emission computed tomography of the head with ^{99m}Cc and a scintillation camera. J Nucl Med 18:373-380, 1977
31. Phelps ME: What is the purpose of emission computed tomography in nuclear medicine. J Nucl Med 18:399-402, 1977
32. New PF, Scott WR, Schnur JA, et al: Computed tomography with the EMI scanner in the diagnosis of primary and metastatic intracranial neoplasms. Radiology 114:75-87, 1975
33. Baker HL Jr., Campbell JK, Houser OW, et al: Early experience with the EMI scanner for study of the brain. Radiology 116:327-333, 1975
34. Treves ST, Mitchell KD, Habboush IH: Three dimensional image alignment, registration and fusion. Q J Nucl Med 42:83-92, 1998
35. Mongioj V, Brusa A, Loi G, et al: Accuracy evaluation of fusion of CT, MR, and spect images using commercially available software packages (SRS PLATO and IFS). Int J Radiat Oncol Biol Phys 43:227-234, 1999
36. Schillaci O, Simonetti G: Fusion imaging in nuclear medicine–applications of dual-modality systems in oncology. Cancer Biother Radiopharm 19:1-10, 2004
37. Townsend DW, Cherry SR: Combining anatomy and function: the path to true image fusion. Eur Radiol 11:1968-1974, 2001
38. Swayne LC: Computer-assisted fusion of single-photon emission tomographic and computed tomographic images. Evaluation in complicated inflammatory disease. Invest Radiol 27:78-83, 1992
39. Horger M, Eschmann SM, Pfannenberg C, et al: The value of SPET/CT in chronic osteomyelitis. Eur J Nucl Med Mol Imaging 30:1665-1673, 2003
40. Bar-Shalom R, Yefremov N, Guralnik L, et al: SPECT/CT using 67Ga and 111In-labeled leukocyte scintigraphy for diagnosis of infection. J Nucl Med 47:587-594, 2006
41. Utsunomiya D, Shiraishi S, Imuta M, et al: Added value of SPECT/CT fusion in assessing suspected bone metastasis: comparison with scintigraphy alone and nonfused scintigraphy and CT. Radiology 238:264-271, 2006

42. Filippi L, Schillaci O, Santoni R, et al: Usefulness of SPECT/CT with a hybrid camera for the functional anatomical mapping of primary brain tumors by [Tc^{99m}] tetrofosmin. Cancer Biother Radiopharm 21:41-48, 2006
43. Kramer EL, Noz ME, Sanger JJ, et al: CT-SPECT fusion to correlate radiolabeled monoclonal antibody uptake with abdominal CT findings. Radiology 172:861-865, 1989
44. Even-Sapir E, Keidar Z, Sachs J, et al: The new technology of combined transmission and emission tomography in evaluation of endocrine neoplasms. J Nucl Med 42:998-1004, 2001
45. Yamamoto Y, Nishiyama Y, Monden T, et al: Clinical usefulness of fusion of 131I SPECT and CT images in patients with differentiated thyroid carcinoma. J Nucl Med 44:1905-1910, 2003
46. Ruf J, Lehmkuhl L, Bertram H, et al: Impact of SPECT and integrated low-dose CT after radioiodine therapy on the management of patients with thyroid carcinoma. Nucl Med Commun 25:1177-1182, 2004
47. Pfannenberg AC, Eschmann SM, Horger M, et al: Benefit of anatomical-functional image fusion in the diagnostic work-up of neuroendocrine neoplasms. Eur J Nucl Med Mol Imaging 30:835-843, 2003
48. Krausz Y, Keidar Z, Kogan I, et al: SPECT/CT hybrid imaging with 111In-pentetreotide in assessment of neuroendocrine tumours. Clin Endocrinol (Oxf) 59:565-573, 2003
49. Amthauer H, Denecke T, Rohlfing T, et al: Value of image fusion using single photon emission computed tomography with integrated low dose computed tomography in comparison with a retrospective voxel-based method in neuroendocrine tumours. Eur Radiol 15:1456-1462, 2005
50. Profanter C, Prommegger R, Gabriel M, et al: Computed axial tomography-MIBI image fusion for preoperative localization in primary hyperparathyroidism. Am J Surg 187:383-387, 2004
51. Schillaci O: Functional–anatomical image fusion in neuroendocrine tumors. Cancer Biol Radiopharm 19:129-134, 2004
52. Schettino CJ, Kramer EL, Noz ME, et al: Impact of fusion of indium-111 capromab pendetide volume data sets with those from MRI or CT in patients with recurrent prostate cancer. Am J Roentgenol 183:519-524, 2004
53. Slomka PJ: Software approach to merging molecular with anatomic information. J Nucl Med 45 Suppl 1:36S-45S, 2004
54. Keidar Z, Israel O, Krausz Y: SPECT/CT in tumor imaging: technical aspects and clinical applications. Semin Nucl Med 33:205-218, 2003
55. Butler T, Hirsch LJ, Claassen J: The hazards of lack of co-registration of ictal brain SPECT with MRI: A case report of sinusitis mimicking a brainstem seizure focus. BMC Nucl Med 4:2, 2004
56. Wahl RL: Why nearly all PET of abdominal and pelvic cancers will be performed as PET/CT. J Nucl Med 41:82S-95S, 2004 (suppl 1)